A Domino Aldol Addition/Hemiketal Formation/Hemiketal Formation/ Epimerization Route to a Heteroadamantane. A Crystal-Structure, NMR, and Computational Study

by **Horst Glaser**[a]), **Ralph Puchta**[a]), **Nico J. R. van Eikema Hommes**[a]), **Dirk Leusser**[b]), **Alexander Murso**[b]), **Dietmar Stalke***[b]), **Walter Bauer***[a]), and **Rolf W. Saalfrank***[a])

[a]) Institut für Organische Chemie, Universität Erlangen-Nürnberg, Henkestrasse 42, D-91054 Erlangen (e-mail: bauer@organik.uni-erlangen.de; saalfrank@organik.uni-erlangen.de; phone: +49-9131-8522991 (*W. B.*); +49-9131-8522554 (*R. W. S.*); fax: +49-9131-8522991)

[b]) Institut für Anorganische Chemie, Universität Würzburg, Am Hubland, D-97074 Würzburg (e-mail: dstalke@chemie.uni-wuerzburg.de; phone: +49-931-8884783; fax: +49-931-8884619)

Dedicated to Professor Dr. Dr. h.c. *Dieter Seebach* on the occasion of his 65th birthday

It has been found by serendipity during the attempted synthesis of the potential tris-bidentate ligand **7** that this compound undergoes multiple ring-closure reactions to form the heterodamantane derivative **12**. This reaction involves a domino aldol addition/hemiketal formation/hemiketal formation/epimerization sequence. Compound **12** was studied intensively by X-ray crystal-structure analysis, NMR, and AM1 computations. Complete assignment of all ^{1}H- and ^{13}C-NMR signals was achieved by a combination of HMQC, HMBC, DPFGSE-NOE, COSY, and long-range-COSY experiments. The NMR data agreed well with the crystallographic and computational results. Accordingly, **12** is present as the thermodynamically most-stable diastereoisomer with relative *u*-configuration at centers C(8) and C(9). In summary, five stereogenic centers were created starting from an achiral precursor in an efficient cascade reaction under thermodynamic control.

Introduction. – The fundamental moiety of adamantane (**1**) is found in numerous heteroatom analogs such as azaadamantane (**2**) and urotropine (**3**) [1][2]. These types of compounds are of particular interest both from a scientific point of view as well as for industrial organic syntheses. Heteroatom analogs of adamantane are found in natural products, *e.g.*, in the extremely toxic pufferfish tetrodotoxine (**4**) [3] (lethal dose for man *ca.* 1 mg). We report here the synthesis of the new dioxaazaadamantane derivative **12**.

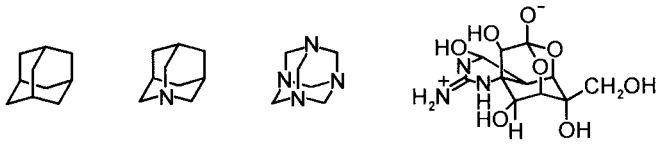

1 **2** **3** **4**

Results. – *Synthesis.* As part of our current research, we were interested in the synthesis of new tris-bidentate ligands. Starting from nitrilotriacetic acid triethyl ester (**5**) we expected that reaction with pinacolone (**6**) would lead in a *Claisen* condensation to tris(5,5-dimethyl-2,4-dioxohexyl)amine (**7**; H_3L) (*Scheme 1*). The tris-enolate (L^{3-}) of **7** should be potentially suitable for complexation of appropriate metal ions, leading

Scheme 1

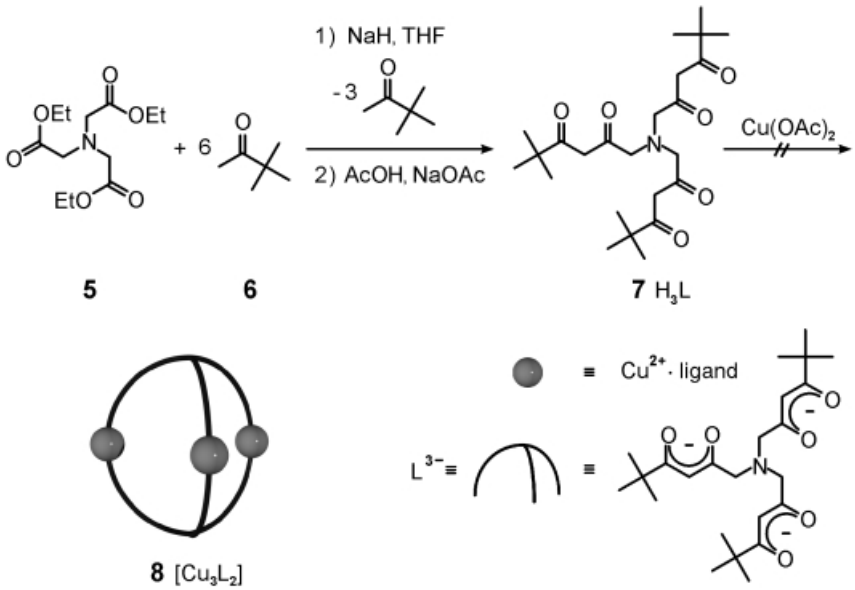

to higher aggregated clusters. Therefore, we planned to react **7** with copper(II) acetate to obtain the trinuclear complex $[Cu_3L_2]$ **8** (*Scheme 1*). Similar examples of complexes of type **8** have been described before by our group [4–6].

The procedure lined out for the preparation of **7** (*Scheme 1*) at first seemed to proceed in a routine way. However, the product obtained after chromatography (silica gel) showed puzzling NMR spectra not compatible with the expected structure **7**. Finally, the structure of the product obtained was determined to be the dioxaazaadamantane **12**. It is self-evident that, due to the achiral reaction conditions, both enantiomers of **12** were obtained as a racemate. Results of the crystal structure determination and NMR experiments of **12**, as well as calculations on the intermediates **9**–**11** of the reaction sequence and on product **12** (*Scheme 2*) are reported. For convenience, we refer in the following discussion only to the enantiomers depicted.

NMR Studies. The IUPAC name for compound **12** is 1-[5-(3,3-dimethyl-2-oxobutyl)-10-(2,2-dimethylpropionyl)-7-hydroxy-4,6-dioxa-1-azatricyclo[3.3.1.1^{3,7}]dec-3-yl]-3,3-dimethylbutan-2-one[1]). However, and for convenience, we refer throughout this paper to the particular enantiomer of **12** and to the arbitrary numbering shown in *Fig. 1*.

Moreover, we assign the diastereotopic protons in **12** at C(14) and C(18) as *pro-r* and *pro-s* as depicted in *Fig. 1*. This arbitrary notation (correct symbols would be *pro-R* and *pro-S*) should symbolize that the assignments at these positions do not change when going from one enantiomer of **12** to the other. The assignments as *pro-R* and *pro-S* of the diastereotopic protons at C(2), C(6), and C(10) are reflection-variant. To avoid

---

[1]) The name was generated by *Beilstein's* 'AutoNom Software' [7].

Scheme 2

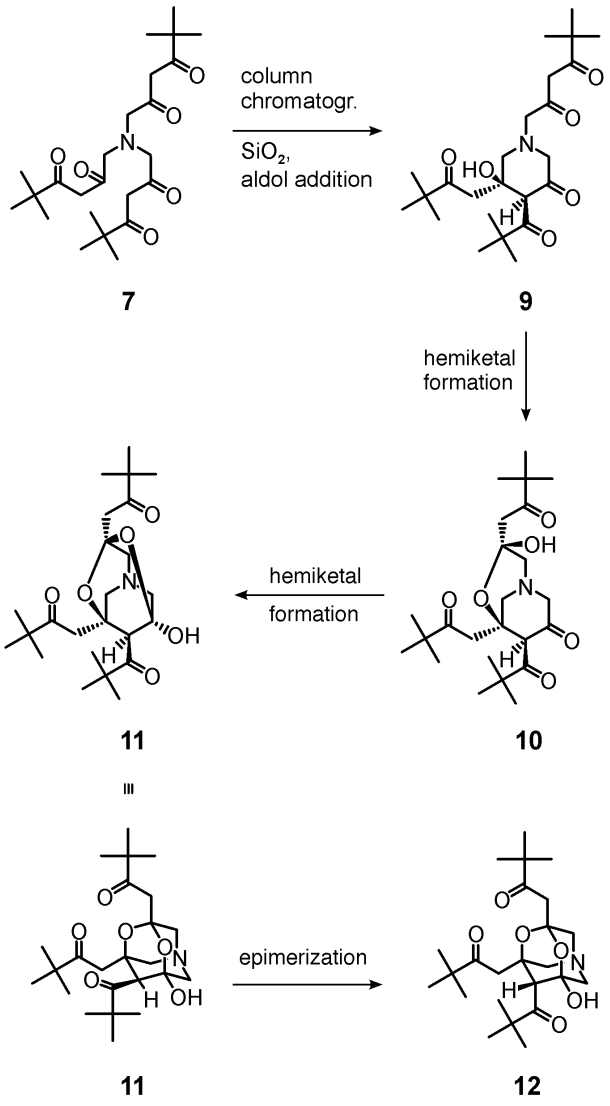

any confusion, we do not denote them as *pro-R* and *pro-S*. Instead, we employ the arbitrary notations a (for axial) and e (for equatorial). It is self-evident that, in adamantane and its derivatives, there are no genuine axial and equatorial positions.

Compound **12**, when prepared according to *Schemes 1* and *2*, affords surprisingly clean ^{1}H- and ^{13}C-NMR spectra. No by-products and impurities are observed, and the spectra show the presence of only a single diastereoisomer of **12**. This is remarkable with respect to the energies of the different species that could principally be formed. We will discuss this in the '*Computational Studies*' section below.

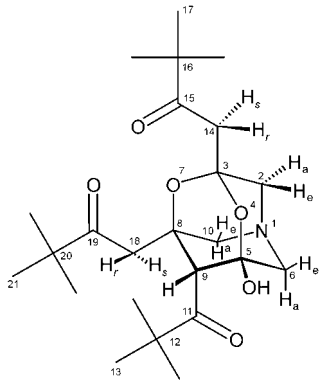

12

Fig. 1. *Structural formula of* **12** *with arbitrary numbering as employed in the text, in the NMR spectra, and in the calculated structures.* For the IUPAC name, see text. Notations *r* and *s* refer to prochiral H-atoms. Notations e and a refer to arbitrarily assigned equatorial and axial positions.

The spectral assignments involved analysis by a combination of COSY, HMQC, HMBC, and NOE experiments. The analysis of the standard COSY and HMQC data is straightforward and will not be discussed any further.

Fig. 2 shows the HMBC spectrum of **12**, indicative of ^2J and ^3J ^{1}H,^{13}C-couplings.

In the 1D ^{1}H-NMR spectrum of **12** (see *Figs. 2* and *3*), the signal of H–C(9) appears as a *t* with $J = 1.9$ Hz. This splitting is due to W-type coupling across four bonds with H_e–C(6) and H_e–C(10). The W-coupling is a first indication of the configuration at C(9) as indicated in *Fig. 1* (equatorial position of H–C(9)). The W-coupling of H–C(9) is confirmed by the appropriate cross-peaks in the long-range-COSY plot (*Fig. 3*).

Proton H–C(9) is the starting point for the spectral assignment of the remaining ^{1}H- and ^{13}C-NMR signals. All quaternary C-atom signals may be unambiguously assigned from the HMBC spectrum shown in *Fig. 2*. In addition, *via* linkage by the cross-peaks of the carbonyl signals, the assignment of the resonance lines of the three nonequivalent *t*Bu groups is achieved.

When processed with resolution enhancement (*Gauss* window), the 1D ^{1}H-NMR spectrum of **12** displays additional splittings for the signals of H_a, H_e–C(2), H_a, H_e–C(6), H_a, H_e–C(10) (*cf. Fig. 3*). These arise from W-type couplings: ^4J(2e,10a) = 1.0 Hz, ^4J(2a,6a) = 1.0 Hz, ^4J(9,10e) = 1.9 Hz, ^4J(6e,10e) = 1.3 Hz, and ^4J(6e,9) = 1.9 Hz. Thus, the signals of the diastereotopic protons at C(2) may be assigned by means of the long-range-COSY plot (*Fig. 3*). These assignments are confirmed by the NOE data (see below).

The ^{13}C-NMR chemical shifts of **12** are in complete agreement with the proposed structure shown in *Fig. 1*. The *Table* shows a comparison of the experimentally obtained δ (C) with data predicted by the 'CSEARCH Software' provided by *Robien* [8]. The constantly higher experimental shift values may be attributed to solvent effects and to referencing discrepancies.

To further validate the hitherto gained assignments, a series of ^{1}H-NOE spectra was recorded. The field-gradient-based pulse sequence DPFGSE-NOE [9] was employed. Each ^{1}H-NMR resonance line of **12** was examined separately. A selection of typical spectra is collected in *Fig. 4*.

Excitation of H–C(9) (*Fig. 4,b*) results in a weak NOE at the HDO signal. This is due to a transferred NOE from the genuine OH resonance of **12** at δ 9.18 (not shown in *Fig. 4*). In addition, the expected medium NOE to Me(13) of the *t*Bu group arises. The NOEs to Me(17) and Me(21) of the *t*Bu groups are very weak (0.1 and 0.2%, resp.). This may be taken as evidence of the equatorial position of H–C(9) as shown in *Fig. 1*. In the case that H–C(9) was in the axial position, a much more intense NOE to Me(21) of the *t*Bu group should result. *Fig. 4,b* shows an additional medium NOE to one of the diastereotopic protons of CH_2(18). Along with the preferred conformation in the crystal structure (see below), this resonance line may be assigned to the *pro-r* proton.

Selective excitation of H_a–C(10) (*Fig. 4,c*) results in a very weak (0.1%) NOE for H–C(9). Again, this is further evidence of the equatorial, 'remote' position of H–C(9). Excitation of H_e–C(6) (*Fig. 4,d*) leads to a

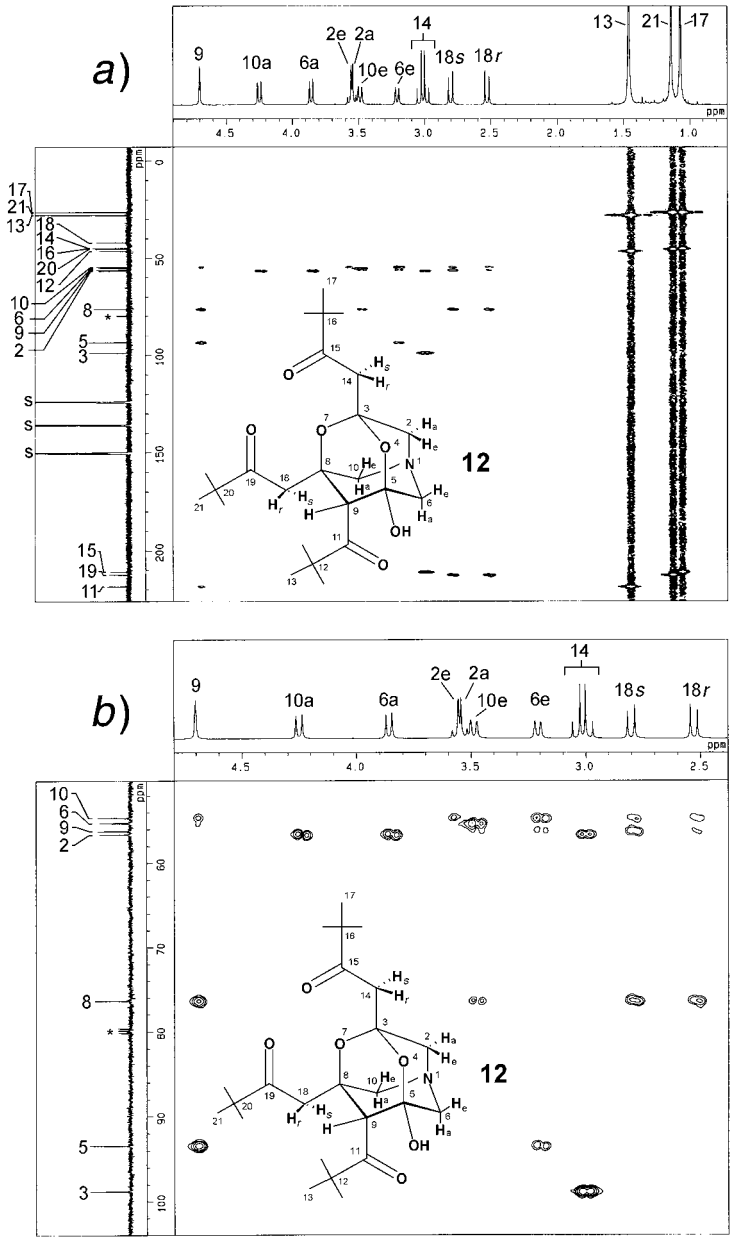

Fig. 2. *Field-gradient $^{1}H,^{13}C$-HMBC spectrum of* **12** ((D_5)pyridine, $+24°$). a) *full range*; b) *zoomed region*. Numbering according to *Fig. 1*. s = solvent signals; * = signal of residual $CDCl_3$. Cross-peaks buried in the t_1-noise ridges are clearly visible when cut at a higher threshold.

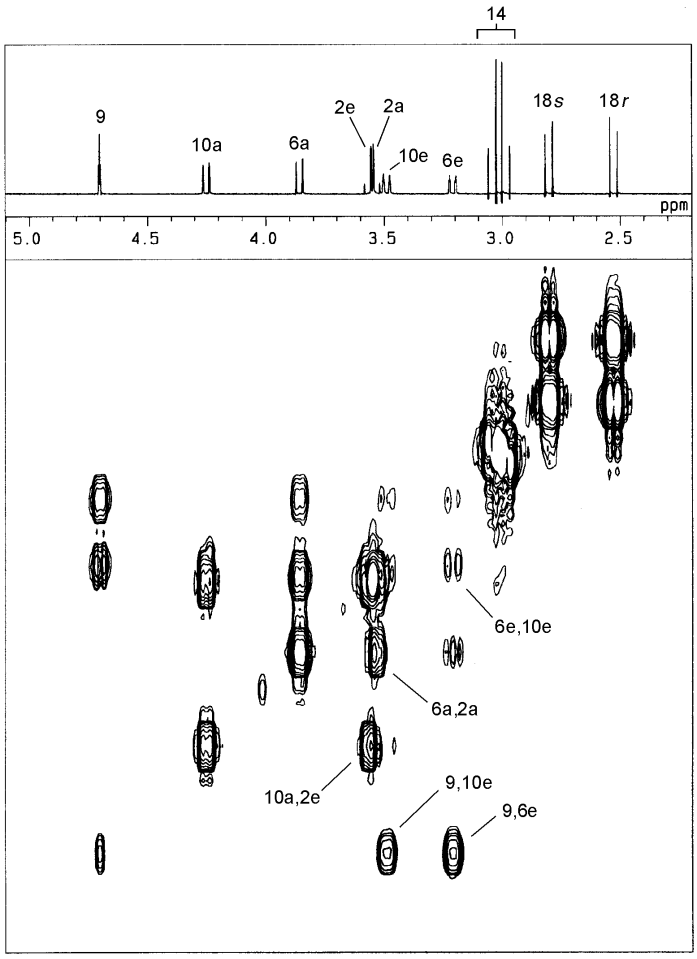

Fig. 3. *COSY Data of* **12** ((D$_5$)pyridine, +24°), *optimized for long-range couplings* (see *Exper. Part*). The assignments in the 1D spectrum refer to *Fig. 1*. In the 2D plot, assignments refer to ^4J-couplings. The 1D spectrum was processed with resolution enhancement (*Gauss* window). The contour plot shows a zoomed region of the total spectrum.

Table 1. *Comparison of Experimental* ^{13}*C-NMR Chemical Shifts of* **12** *with Calculated Values from the 'CSEARCH Software'* [8]. The keyword 'HOSE3D' was employed. The assignment is as shown in *Fig. 1*.

	δ exper.	δ calc.		δ exper.	δ calc
C(11)	218.4	209.9	C(10)	54.7	51.5
C(19)	212.4	207.9	C(12)	46.4	44.7
C(15)	210.9	210.6	C(20)	45.4	43.9
C(3)	98.8	99.5	C(16)	45.1	43.9
C(5)	93.4	99.5	C(14)	45.0	35.6
C(8)	76.3	74.7	C(18)	42.1	35.6
C(2)	56.6	51.5	C(13)	28.0	26.2
C(9)	56.2	47.6	C(21)	26.6	26.2
C(6)	55.3	51.5	C(17)	26.5	26.2

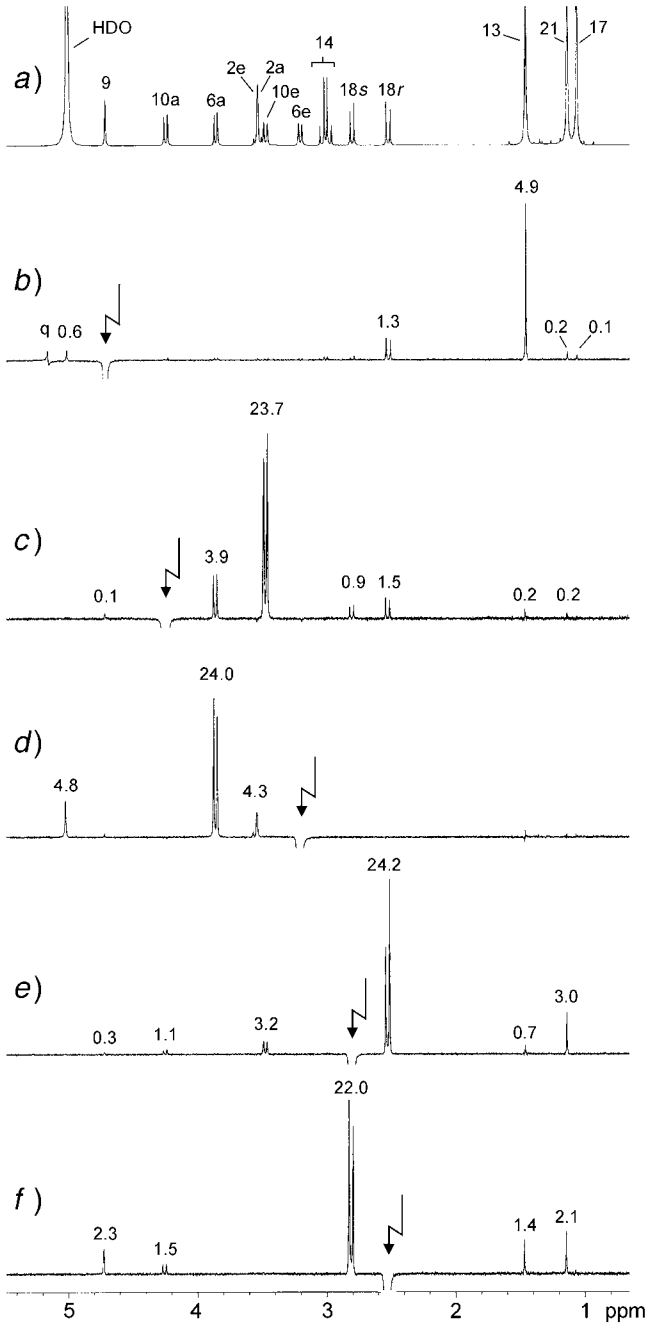

Fig. 4. *^{1}H-NOE Data of* **12** ((D$_5$)pyridine, +24°), pulse sequence: DPFGSE-NOE): a) *normal ^{1}H-NMR spectrum, assignments as in* Fig. 1; b)–f) *NOE plots with selective* Gaussian *excitation pulses at positions indicated by an arrow.* Assignments in *a*) refer to *Fig. 1*. Values in *b*)–*f*) are percentage enhancements, scaled to the irradiated signal intensity = –100%. No scaling for numbers of involved protons has been made. Symbol q in *b*) denotes an artificial quad-image of the irradiated position.

medium NOE (4.3%) at the low-field resonance of the diastereotopic protons $CH_2(2)$, which must consequently be assigned to $H_e-C(2)$. This is in agreement with the above results obtained from analysis of the ^4J coupling constants.

When the low-field line of the diastereotopic protons $CH_2(18)$ is irradiated (*Fig. 4,e*), weak to medium NOEs are observed for $H_a-C(10)$ and $H_e-C(10)$ (1.1 and 3.2%, resp.), thus assigning $H_s-(18)$. This observation suggests a different preferred conformation of the residue at C(8) as compared to the calculated structure (see below, *Fig. 7*). However, these NMR results are in accordance with the positions of the atoms with the major site-occupation factors for the disordered carbonyl function at C(19) found in the solid-state structure of **12** (see below, *Fig. 8,b*). Finally, excitation of $H_r-C(18)$ (*Fig. 4,f*) shows the expected NOEs for H–C(9), $H_a-C(10)$, and Me(13) and Me(21) of the ^{t}Bu groups.

Computational Studies. To corroborate the experimental NMR results, we calculated the structures of the reaction pathway shown in *Scheme 2* at the AM1 level [10] using the 'VAMP7' software package [11].

All steps of the domino aldol additon/hemiketal formation/hemiketal formation/epimerization mechanism are exothermic (starting amine **7**: $\Delta H_f^0 = -254.0$ kcal/mol). The initial aldol addition (formation of **9**) liberates *ca.* 75% of the total energy of the pathway. Principally, two diastereoisomers may be formed (*Fig. 5,a* and *b*). The diastereoisomer of *Fig. 5,a* is considerably more stable than the diastereoisomer of *Fig. 5,b* (−260.1 *vs.* −254.7 kcal/mol). This is largely due to steric reasons originating from the bulky ^{t}Bu groups. An additional stabilization in the diastereoisomer of *Fig. 5,a* is gained from H-bonding between the newly formed OH group and the adjacent C=O group (dashed line in *Fig. 5,a*). The diastereoisomer shown in *Fig. 5,a* has the (*R*) configuration at C(8) and at C(9) (relative *l*-configuration) [12] [13].

In the second reaction step (*Scheme 2*), the newly formed OH group from the aldol-addition step attacks a carbonyl group of the remaining 'free' residue at the N-atom of **9**, thus forming hemiketal **10**. It is self-evident that this step involves the formation of a third stereogenic center. We have calculated only those diastereoisomers of **10** with a configuration at the new stereogenic center that may lead to the final heteroadamantane. Of the two diastereoisomers with OH groups in the correct 'frontside' position, the species with similar configuration as for **9** (8*R*) and (9*R*) turned out to be more stable than the corresponding *u*-isomer (−262.8 *vs.* −258.2 kcal/mol; *Fig. 6*).

The presentations of the molecular structures of **10** (*Fig. 6*) indicate preformation of the final heteroadamantane skeleton. The OH group is in vicinity to the carbonyl group attacked in the next, second hemiketal-forming step. Thus, there is only one choice for the configuration of the newly created stereogenic center at this stage, eventually leading to heteroadamantane **12** (*Fig. 7,b*). The calculations show that heteroadamantane **11** with retained (8*R*, 9*R*) configurations at C(8) and C(9) is less stable than epimer **12** with configuration (8*R*, 9*S*) (relative *u*-configuration). Without doubt, this is due to steric interactions of the bulky residues at C(8) and C(9). As a consequence, a final epimerization reaction at C(9) takes place. Since all involved steps (aldol addition, hemiketal formation, epimerization) are reversible reactions, the epimerization at C(9) appears to be a plausible process. Thus, the calculations are in complete agreement with the experimental results and confirm the suggested reaction pathway outlined in *Scheme 2*.

X-Ray-Structure Determination. Colorless crystals of compound **12** were obtained by slow evaporation of a solution of **12** in (D_5)pyridine. The compound crystallized as a merohedrical twin in the chiral space group $I4_1$. *Fig. 8,a*, establishes that the solid-state

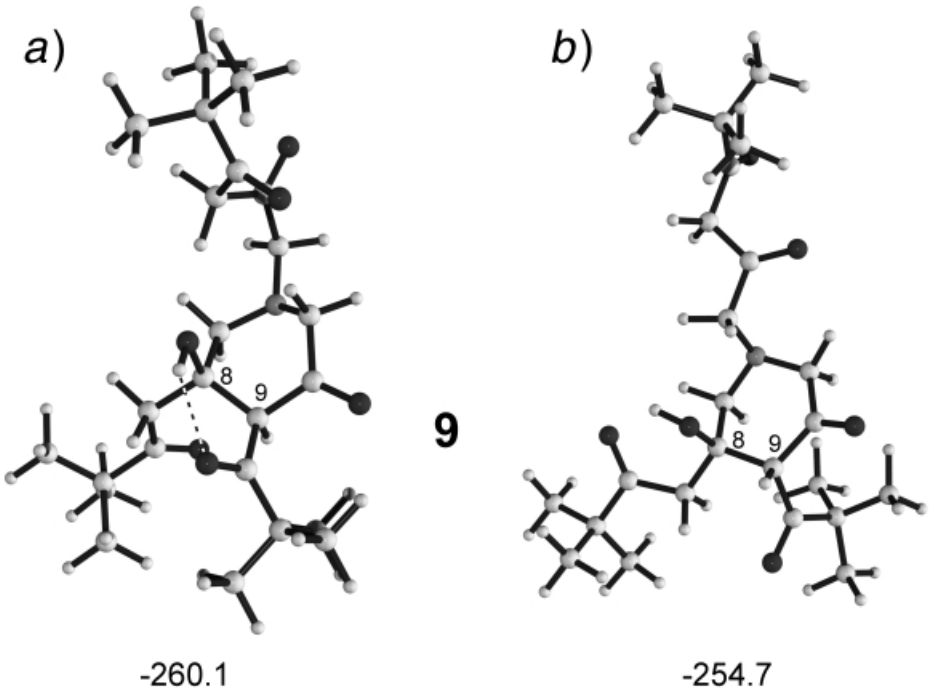

Fig. 5. *AM1-Calculated structures of* **9**: a) l-*epimer with respect to C(8) and C(9)* (residues with ^{t}Bu groups in *anti*-position); b) u-*epimer with respect to C(8) and C(9)* (residues with ^{t}Bu groups in *syn*-position). Values below structures are heats of formation ΔH_f^0 [kcal/mol].

structure of **12** is in accordance with the structure in solution deduced from the solution NMR studies, with both the H–C(9) (= H9) and H-atom of the hydroxyl function (= H99) being arranged equatorially. *Fig. 8,b* shows the detected disorder of the substituent at C(8) of the heteroadamantane core. The positions of the atoms with minor site-occupation factor (0.21) are transparent. Taking this disorder into account, the assignment of H_s–C(18) in the NOE experiment displayed in *Fig. 4,f* is correct for the positions of atoms with the major site-occupation factors.

As expected from the space-group symmetry $I4_1$, the molecules are arranged along the 4_1-screw axis in helical strands. *Fig. 9* depicts the aggregation of the molecules linked by two different types of intermolecular H-bonds. First, the hydroxy H-atom H99A of one molecule is connected to the amine N-atom N1B of another molecule at a distance of 190.5 pm, indicating a strong interaction [15]. In addition, one of the acidic H-atoms (H14C) of the methylene group CH_2(14) (= C14C) is bound to the carbonyl O-atom (O3D) of the other molecule at a distance of 249.1 pm, which is in the range of distances found for weak C–H···O H-bonds (*Fig. 9*) [15].

Conclusions. – We have described in detail the NMR and computational properties along with the crystal structure of the new heteroadamantane **12**. The formation of this compound was found by serendipity: in an efficient cascade reaction, the initially attempted amine **7** underwent an aldol addition, two hemiketal formations, and an

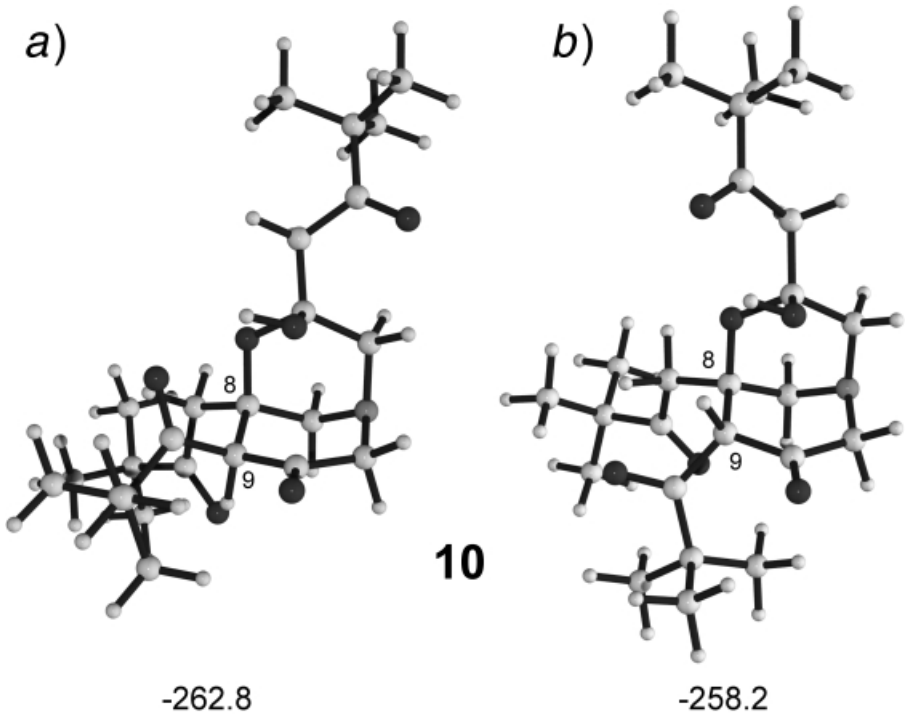

Fig. 6. *AM1-Calculated structures of* **10**: a) l-*epimer with respect to C(8) and C(9)* (residues with ^{t}Bu groups in *anti*-position); b) u-*epimer with respect to C(8) and C(9)* (residues with ^{t}Bu groups in *syn*-position). Values below structures are heats of formation ΔH_f^0 [kcal/mol].

epimerization step to form heteroadamantane **12** in a remarkably clean way. No diastereoisomers of **12** were detected by NMR. In summary, when starting from an achiral precursor **7**, *five* (!) new stereogenic centers (including at a N-atom) were formed from scratch. Of the principally $2^5 = 32$ isomers, only the racemic mixture of **12** was found. This must be a consequence of the reversibility of the reactions involved, leading *via* thermodynamic control to the most-stable diastereoisomer **12**. We consider these remarkable findings to be a further impressive example of the power of cascade reactions.

The authors gratefully acknowledge financial support by the *Deutsche Forschungsgemeinschaft* and the *Fonds der Chemischen Industrie.*

Experimental Part

General. NMR spectra: *Jeol Alpha500* spectrometer (^{1}H at 500.1 MHz); (D_5)pyridine soln.; chemical shifts δ in ppm rel. to $SiMe_4$ (= 0 ppm) referenced to the solvent signals: δ(H) 7.22 and δ(C) 123.8, J in Hz; samples of **12** were carefully degassed before measurement. The following spectral parameters were used. *Fig. 2:* HMBC, field-gradient mode, inverse probehead, 90° pulses 6.0 μs (^{1}H) and 15.5 μs (^{13}C), spectral width in $f_2 = 4623$ Hz, spectral width in $f_1 = 29325$ Hz, 512 data points in f_2, zero-filled to 1024, 512 increments in t_1, zero-filled to 1024, 8 scans per increment, acquisition time 0.11 s, relaxation delay 2.0 s, exponential window in t_2 and *Gaussian*

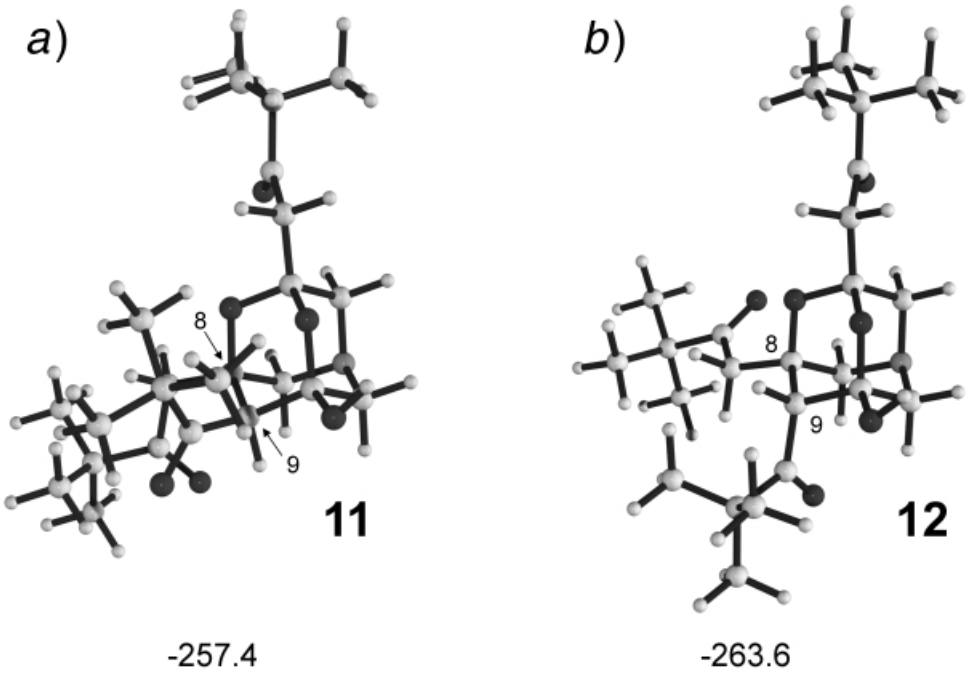

Fig. 7. *AM1-Calculated structures of* a) **11**: (*l*-epimer with respect to C(8) and C(9), residues with ^{t}Bu groups in *anti*-position), *experimentally not found*, and b) **12** (*u*-epimer with respect to C(8) and C(9), residues with ^{t}Bu groups in *syn*-position), *experimentally found*. The orientation of the heteroadamantane moieties is as shown in *Fig. 1*. Values below structures are heats of formation ΔH_f^0 [kcal/mol].

window in t_1. *Fig. 3:* COSY for long-range couplings; inverse probehead with 90° ^{1}H-pulse width as for *Fig. 2*, acquisition time 0.11 s, relaxation delay 2.0 s, spectral width in f_1 and f_2 = 4623 Hz, 512 data points in f_2, zero-filled to 1024, 128 data points in f_1, zero-filled to 512, unshifted sine bell window in both dimensions; a constant delay of 200 ms is introduced before and after the second 90° pulse of the standard COSY pulse sequence. *Fig. 4:* DPFGSE-NOE; inverse-field-gradient probehead, pulse sequence as in [14], spectral width 4623 Hz, 16384 data points, hard 90° pulse width 6.3 μs, 180° soft *Gaussian* pulse width 40 ms, 512 scans per irradiation point with additional 32 pre-dummy scans, acquisition time 3.54 s, relaxation delay 2.0 s, mixing time 500 ms, gradient strengths 19.6/8.4/5.6/ − 5.6 G/cm, exponential weighting (BF = 0.2 Hz).

Compound **12**. To a stirred suspension of NaH (12.0 mmol, 288 mg) in dry THF (50 ml), a soln. of 1,1-dimethylpropan-2-one (12.0 mmol, 1.20 g) in dry THF (25 ml) was added within 15 min. After stirring for 1 h, a soln. of nitrilotriacetic acid triethyl ester (2.00 mmol, 551 mg) in dry THF (25 ml) was added dropwise to the mixture within 1 h. The mixture was stirred for 6 h at r.t. and for 16 h under reflux and then cooled for 3 h to − 18°. The precipitated solid was filtered off, washed with Et_2O, and added to an aq. AcOH/NaOAc buffer (1M, 100 ml/8.20 g). After stirring for 1 h, the AcOH soln. was extracted with $CHCl_3$ (4 × 30 ml). The combined org. extract was dried (Na_2SO_4), concentrated to 5 ml, and purified by column chromatography (SiO_2, AcOEt; R_f = 0.96). Within 2 days, an amber solid precipitated from an AcOEt soln., which was filtered off, washed with Et_2O and dried *in vacuo:* 234 mg (26.7%) of **12**. M. p. 164°. IR ($CHBr_3$): 2967 (C−H) 1711, 1680 (C=O). ^{1}H-NMR (500 MHz, C_5D_5N; numbering according to *Fig. 1*): 1.07 (*s*, ^{t}Bu (Me(17))); 1.15 (*s*, ^{t}Bu (Me(21))); 1.47 (*s*, ^{t}Bu (Me(13))); 2.53 (*d*, ^2J(H,H) = 15.5, H$_r$−C(18)); 2.81 (*d*, ^2J(H,H) = 15.5, H$_s$−C(18)); 2.99 (*d*, ^2J(H,H) = 16.4, 1 H−C(14)); 3.05 (*d*, ^2J(H,H) = 16.4, 1 H−C(14)); 3.21 (*ddd*, ^2J(H,H) = 13.0, ^4J(H,H) = 1.3, 1.9, H$_e$−C(6)); 3.48 (*ddd*, ^2J(H,H) = 13.6, ^4J(H,H) = 1.3, 1.9, H$_e$−C(10)); 3.53 (*dd*, ^2J(H,H) = 13.4, ^4J(H,H) = 1.0, H$_a$−C(2)); 3.56 (*dd*, ^2J(H,H) = 13.4, ^4J(H,H) = 1.0, H$_e$−C(2)); 3.87 (*dd*, ^2J(H,H) = 13.0, ^4J(H,H) = 1.0, H$_a$−C(6)); 4.26 (*dd*, ^2J(H,H) = 13.6, ^4J(H,H) = 1.0, H$_a$−C(10)); 4.73 (*dd*, ^4J(H,H) = 1.9, 1.9, H−C(9)); 9.18 (br. *s*, OH). ^{13}C{^{1}H}-

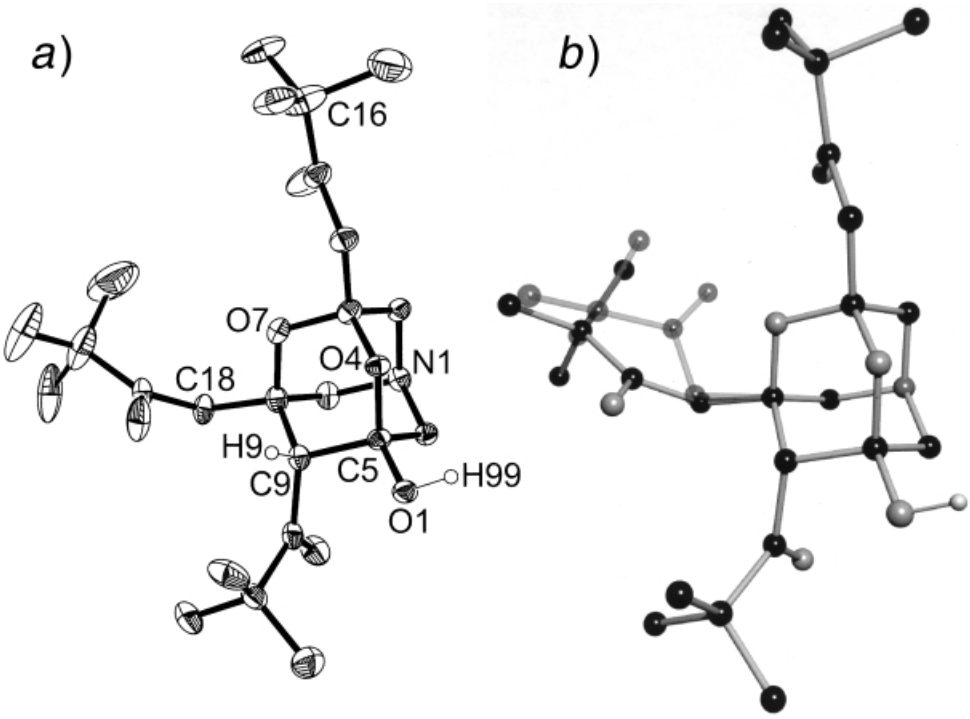

Fig. 8. a) *Solid-state structure of* **12** (anisotropic displacement parameters depicted at the 50% probability level; disordered atoms omitted for clarity); b) *ball-and-stick diagram of* **12** *with disordered* ^{t}BuC(=O) group at C(18) (minor site-occupation factors transparent (0.15))

NMR (125 MHz, C_5D_5N; numbering according to *Fig. 1*): 26.47 (C(17)); 26.55 (C(21)); 27.98 (C(13)); 42.08 (C(18)); 44.98 (C(14)); 45.10 (C(16)); 45.38 (C(20)); 46.39 (C(12)); 54.67 (C(10)); 55.29 (C(6)); 56.24 (C(9)); 56.27 (C(2)); 76.33 (C(8)); 93.44 (C(5)); 98.81 (C(3)); 210.90 (C(15)); 212.41 (C(19)), 218.41 (C(11)). EI-MS: 437 (24, M^+). Anal. calc. for $C_{24}H_{39}NO_6$ (437.58): C 65.88, H 8.98, N 3.20; found: C 64.80, H 8.91, N 3.09.

Crystal Data and Structure Determination for **12**. The data set was collected at 100(2) K with an oil-coated shock-cooled crystal of size $0.4 \times 0.4 \times 0.2$ mm on a *Bruker APEX-CCD* diffractometer with Mo-K_α (λ 71.073 pm) radiation equipped with a low-temperature device [16]. Reflections were measured to $\theta_{max.} = 25.03°$. The structure was solved by direct methods ('SHELXS-NT 97') [17] and refined by full-matrix least-squares methods against F^2 ('SHELXL-NT 97') [18]. R values defined as $R^1 = \Sigma \| F_o | - | F_c \| / \Sigma | F_o |$, $wR^2 = [\Sigma w(F_o^2 - F_c^2)^2 / \Sigma w(F_o^2)^2]^{0.5}$, $w = [\sigma^2(F_o^2) + (g_1P)^2 + g_2P]^{-1}$, $P = 1/3[\max(F_o^2, 0) + 2F_c^2]$. An empirical absorption correction was applied by means of 'SADABS 2.0' (T_{min} 0.893441, T_{max} 1.00000) [19].

Compound **12** ($C_{24}H_{39}NO_6$, M 437.56) crystallizes as a merohedrical twin in the tetragonal space group $I4_1$ with $a = b = 267.735(13)$ pm, $c = 136.696(9)$ pm, $V = 9.7986(9)$ nm^3, $Z = 16$, $\rho_{cal.} = 1.186$ Mg/m^3, $\mu = 0.084$ mm^{-1}, and $F(000) = 3808$. The determination of the space group in XPREP gives only one solution, the centrosymmetrical space group $I4_1/a$ with *[E*E-1]* = 0.746. Anisotropic refinement of the structure in $I4_1/a$, however, results in $R_1 = 0.3009$ and $wR_2 = 0.7388$. The ADPs of the ^{t}Bu groups indicated serious disorder. A closer inspection of the statistical values revealed typical warning signs for twinning, *i. e.*, $K = mean(F_o^2)/mean(F_c^2)$ was systematically increased for the reflections with low intensity, for all 'most disagreeable' reflections, F_o was much larger than F_c, and *[E*E-1]* was not suitable for the centrosymmetrical space group $I4_1/a$ [20].

Introduction of the twin matrix 0 1 0 1 0 0 0 0 $\bar{1}$ improved the refinement considerably. This matrix confirms that the *a*-glide plane is only emulated by twinning. The final structure refinement employing all 47111

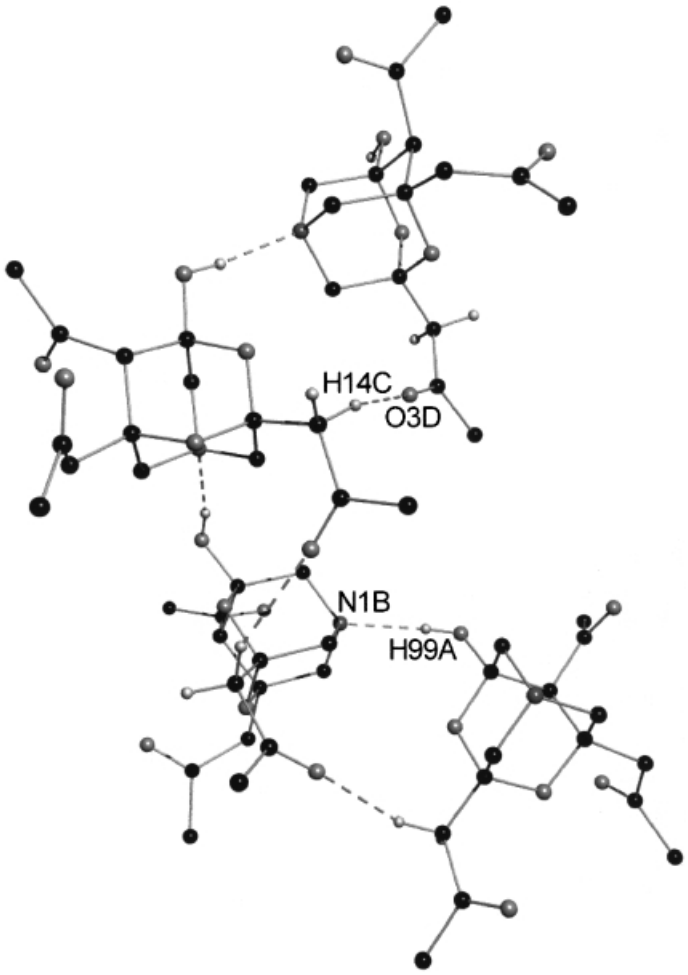

Fig. 9. *Arrangement of* **12** *along the* 4_1*-screw axis and intermolecular H-bonding*. The ^{t}Bu groups are omitted for clarity. Selected bond lengths and angles: H99A···N1B 190.5 pm, O1A–H99A–N1B 169.0°, H14A···O3B 249.1 pm, and C14A–H14A–O3B 151.6°.

measured reflections, of which 4314 were unique, gives the following R values: wR^2(all data) = 0.1179, $R^1(I > 4\sigma(I)) = 0.0433$, $g_1 = 0.0747$, $g_2 = 7.3857$ for 4314 data, 353 restraints, and 384 parameters. The maximal peak and hole in the final difference *Fourier* synthesis is 0.407 and −0.260 eÅ^{-3}. The ^{t}Bu group C17A to C17C, and the residue ^{t}BuC(=O)CH_2 at C(8) are disordered and were refined with distance and ADP restraints. The site-occupation factors of the disordered ^{t}Bu group C17A to C17C refined to 0.58 and 0.42, those of the residue ^{t}BuC(=O)CH_2 at C(8) to 0.79 and 0.21, respectively. All non-H-atoms were refined anisotropically. The position of the H-atoms H99 and H9 were taken from the difference *Fourier* map and refined freely, all other H-atoms were positioned geometrically idealized and refined using a riding model. Crystallographic data for the structure of **12** has been deposited with the *Cambridge Crystallographic Data Centre* as supplementary publication No. CCDC-194039. Copies of the data can be obtained free of charge on application to CCDC, 12 Union Road, Cambridge CB2 1EZ, UK (fax: (internat.) +44-1223/336-033; e-mail: deposit@ccdc.cam.ac.uk).

REFERENCES

[1] H. Stetter, *Angew. Chem.* **1954**, *66*, 217.
[2] H. Stetter, *Angew. Chem.* **1962**, *74*, 361.
[3] W. Davis, *Science (Washington, D.C.)* **1989**, *240*, 1715.
[4] R. W. Saalfrank, N. Löw, S. Kareth, V. Seitz, F. Hampel, D. Stalke, M. Teichert, *Angew. Chem.* **1998**, *110*, 182; *Angew. Chem., Int. Ed.* **1998**, *37*, 172.
[5] R. W. Saalfrank. H. Glaser B. Demleitner, F. Hampel, M. M. Chowdhury, V. Schünemann, A. X. Trautwein, G. B. M. Vaughan, R. Yeh, A. V. Davis, K. N. Raymond, *Chem.–Eur. J.* **2002**, *8*, 493.
[6] E. Uller, B. Demleitner, I. Bernt, R. W. Saalfrank, *Struct. Bonding* **2000**, *96*, 149.
[7] *Beilstein*, 'AutoNom Software', Version 2.02.119.
[8] W. Robien, Institute of Organic Chemistry, University of Vienna (Austria), 'CSEARCH Online Software'; (http://mailbox.univie.ac.at/~robienw8/csearch_server_info.html).
[9] K. Stott, J. Keeler, Q. N. Van, A. J. Shaka, *J. Magn. Reson.* **1997**, *125*, 302.
[10] M. J. S. Dewar, E. G. Zoebisch, E. F. Healy, J. J. P. J. Stewart, *J. Am. Chem. Soc.* **1985**, *107*, 3902.
[11] P. Gedeck, F. Burkhardt, A. Horn, B. Beck, G. Rauhut, A. Alex, J. Chandrasekhar, T. Steinke, W. Sauer, M. Hutter, T. Clark, '*VAMP 7.0*', Oxford Molecular, The Medawar Centre, Oxford Science Park, Sandford-on-Thames, Oxford OX4 4GA, U.K.
[12] D. Seebach, V. Prelog, *Angew. Chem.* **1982**, *94*, 696; *Angew. Chem., Int. Ed.* **1982**, *21*, 654.
[13] V. Prelog, G. Helmchen, *Angew. Chem.* **1982**, *94*, 614; *Angew. Chem., Int. Ed.* **1982**, *21*, 567.
[14] S. Braun, H.-O. Kalinowski, S. Berger, '150 and More Basic NMR Experiments', VCH Weinheim, 1998, p. 460 f.
[15] G. R. Desiraju, T. Steiner, 'The Weak Hydrogen Bond', Oxford University Press, Oxford, 2001; T. Steiner, *Angew. Chem*. **2002**, *114*, 50; *Angew. Chem., Int. Ed.* **2002**, *41*, 48.
[16] T. Kottke, D. Stalke, *J. Appl. Crystallogr*. **1993**, *26*, 615; T. Kottke, R. J. Lagow, D. Stalke, *J. Appl. Crystallogr*. **1996**, *29*, 465; D. Stalke, *Chem. Soc. Rev.* **1998**, *27*, 171.
[17] G. M. Sheldrick, *Acta Crystallogr., Sect. A* **1990**, *46*, 467.
[18] G. M. Sheldrick, 'SHELXL-97', Program for Crystal Structure Refinement, University of Göttingen, 1993.
[19] G. M. Sheldrick, 'SADABS V. 2.0', Program for Absorption Correction, University of Göttingen, 1999.
[20] R. Herbst-Irmer, G. M. Sheldrick, *Acta Crystallogr., Sect. B* **1998**, *54*, 443.

Received June 25, 2002